

High-Velocity Neutral Plasma Jet Formed by Dense Plasma Deflagration

Keith T. K. Loebner, Benjamin C. Wang, Flavio R. Poehlmann,
Yuto Watanabe, and Mark A. Cappelli

Abstract—High-velocity high-energy-density plasma jets are an invaluable tool for studying plasma-material interactions under extreme thermal, physical, chemical, and electrostatic stresses. Such a jet has been generated in an experimental facility utilizing a pulsed plasma deflagration accelerator. Time-averaged and fast-frame-rate intensified charge-coupled device images of the plasma jet are presented, showing a concentrated high-density plasma near the exit that is characterized with laser interferometry.

Index Terms—Plasma accelerators, plasma density, plasma diagnostics, plasma sources.

THE deflagration mode of pulsed coaxial plasma accelerators has been studied for various applications for over 40 years [1]. A plasma accelerator operated in this mode converts a significantly higher fraction of the input energy into directed kinetic energy than traditional pulsed coaxial accelerators. This results in a higher fluence of energetic particles in the form of a hot, dense plasma jet that exits the electrode assembly after establishment of the discharge. In this paper, we present images of a focused high-velocity plasma jet created using such a pulsed coaxial plasma deflagration accelerator, as well as interferometric data confirming the high plasma density suggested by the visible emission.

The basic operation of the deflagration accelerator consists of discharging a variable number of capacitors into a small volume of working gas, such as hydrogen, as it is puffed into the interelectrode region via a fast-rise-time beam valve. Near-instantaneous ionization occurs, and the ionization wave is quasi-stationary in the laboratory frame as process gas continues to be injected into the interelectrode region. This ionization wave broadens into a diffuse current conduction zone that runs the length of the electrodes [2], after the establishment of which a high-velocity plasma jet exits the accelerator at $\sim 100\text{--}200$ km/s [3]. The mechanism of this jet formation and the detailed properties of the jet are not currently well understood.

Manuscript received November 19, 2013; revised March 31, 2014; accepted June 14, 2014. Date of publication July 8, 2014; date of current version October 21, 2014. This work was supported in part by the U.S. Department of Energy, in part by DoD, and in part by the Air Force Office of Scientific Research, National Defense Science and Engineering Graduate Fellowship under Grant 32 CFR 168a.

K. T. K. Loebner, B. C. Wang, Y. Watanabe, and M. A. Cappelli are with the Department of Mechanical Engineering, Stanford University, Stanford, CA 94305 USA (e-mail: kloebner@stanford.edu; bwang17@stanford.edu; yutow@stanford.edu; cap@stanford.edu).

F. R. Poehlmann is with the Fluence, LLC, Newark, CA 94560 USA (e-mail: flaviop@fluencetech.com).

Digital Object Identifier 10.1109/TPS.2014.2332467

The discharge shown in Fig. 1 was produced using eight $14\text{-}\mu\text{F}$ capacitors for a total capacitance of $112\ \mu\text{F}$, charged to 4 kV. The valve plenum pressure was 10 atm of molecular hydrogen, which produced a $2\text{-}\mu\text{g}$ mass bit. The overall inductance of the system was 100 nH. For the line density data in Fig. 2, collected via optical laser interferometry, the total capacitance was $56\ \mu\text{F}$ at a range of charging voltages from 1 to 4.5 kV, with the other parameters unchanged. At the highest charging voltage, the peak discharge current was measured to be 50 kA.

The image in Fig. 1(a) was collected with a Canon EOS Rebel T3i Digital SLR camera with active image stabilization and an exposure time of 5 s, so that the entire discharge cycle was captured in the time-averaged image. The sequence of images in Fig. 1(b) was obtained using a Cordin 220 fast-framing intensified charge-coupled device camera triggered at $2\text{-}\mu\text{s}$ intervals from the onset of breakdown. A helium–neon laser interferometer, such as that described in [4], was used to collect plasma line density data at the axial location shown in Fig. 1(b), 4.5 cm from the exit plane of the accelerator. The probe beam was aligned to pass through the center of the jet, where the plasma density appears to be highest based on the visible emission data in Fig. 1(b).

The structure of the jet visible in Fig. 1 provides insight into the physics governing its formation by the deflagration discharge. The high-density core appears to form directly on the center electrode axis, indicating a pinching effect due to the large self-induced magnetic fields along the central axis resulting from convergent radial current streamlines. This supports the acceleration mechanism suggested by the deflagration model, which attributes the high kinetic energy of the processed gas to the high magnetic pressure gradient across and along the current conduction zone.

Even at the modest pulse energies studied via interferometry (28–567 J/pulse), a high plasma density was measured in the core of the jet. Interferometric data indicates a path-averaged peak line density of up to $6.5 \times 10^{14}\ \text{cm}^{-2}$, which can be combined with the approximate chord length, visible in Fig. 1(a) as ~ 1 cm, to give a nominal plasma density of $6.5 \times 10^{14}\ \text{cm}^{-3}$ and particle flux of $10^{22}\ \text{cm}^{-2}\ \text{s}^{-1}$ at the focus, assuming a homogeneous density distribution along the measured chord. Fig. 2 shows that the peak line density directly correlates to the peak discharge current. This indicates that this jet should be scalable to significantly higher plasma densities, and thus correspondingly higher particle and energy flux.

The images and supporting density data presented in this paper describe key components of the dynamics and

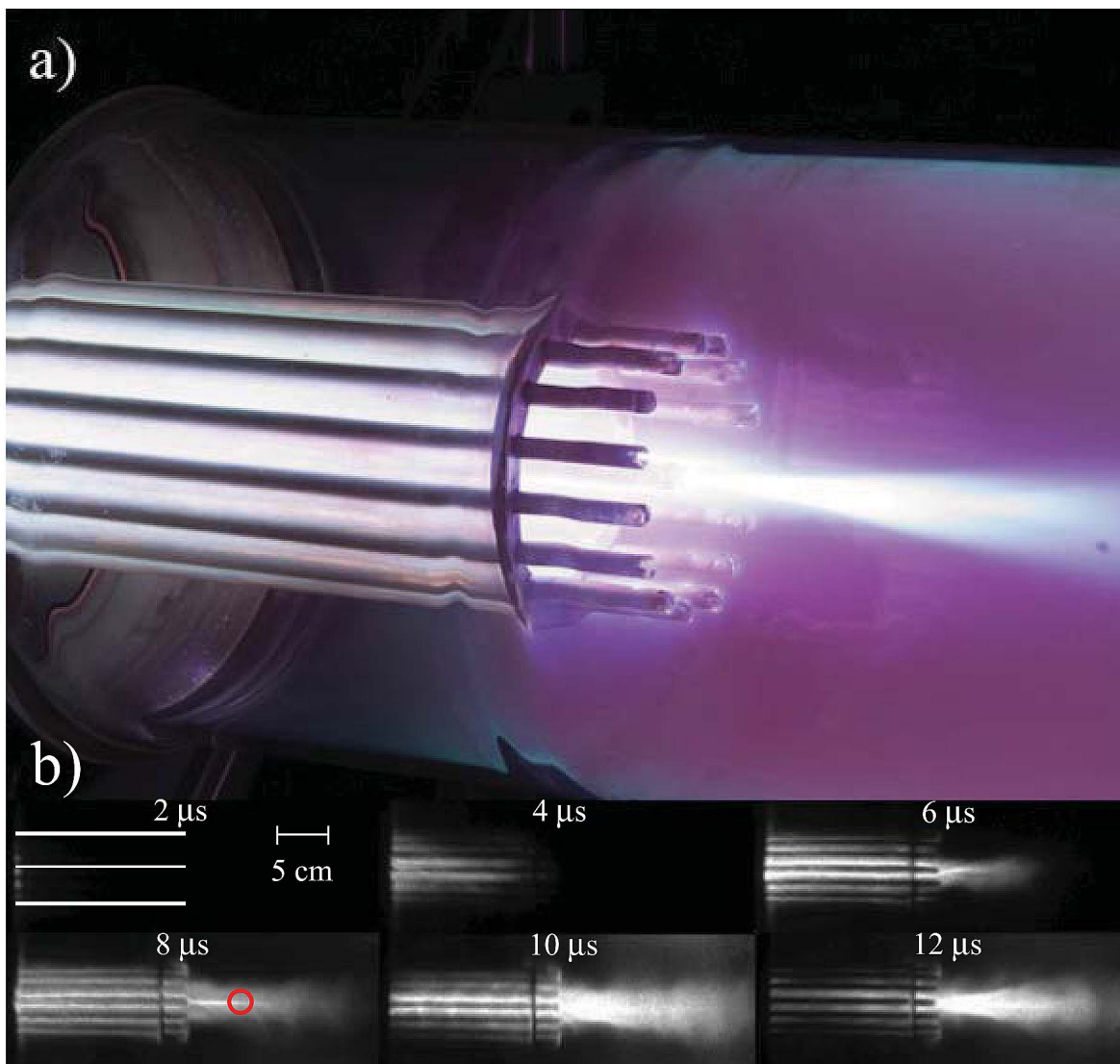


Fig. 1. (a) Time-averaged image of the plasma jet throughout the 20- μ s discharge. (b) ICCD image sequence depicting establishment of deflagration and resulting high-energy jet at 2- μ s intervals starting at breakdown. The accelerator was charged to 4 kV with 112- μ F total capacitance. The red circle indicates the interferometry measurement location; time-resolved data was collected throughout 20- μ s discharge cycle.

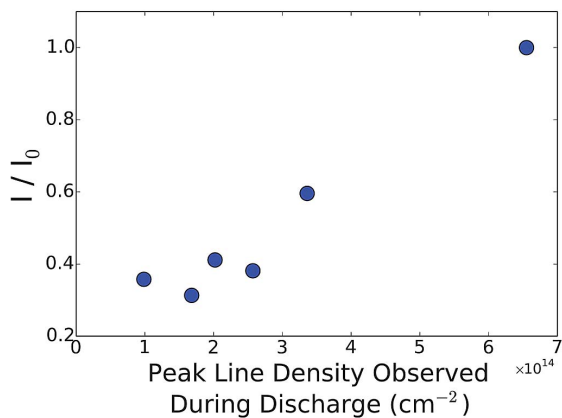


Fig. 2. Plot of interferometric data showing peak observed line density in the core of the jet versus peak discharge current for each test, normalized to the peak observed at 4.5 kV charging voltage ($I_0 = 50$ kA). Absolute density measurements are accurate to within a factor of two.

physical properties of this unique plasma accelerator. This high-velocity dense plasma jet will provide an experimental environment for the examination of extreme plasma-material interactions.

REFERENCES

- [1] D. Y. Cheng, "Plasma deflagration and the properties of a coaxial plasma deflagration gun," *Nucl. Fusion*, vol. 10, no. 3, p. 305, 1970.
- [2] F. R. Poehlmann, M. A. Cappelli, and G. B. Rieker, "Current distribution measurements inside an electromagnetic plasma gun operated in a gas-puff mode," *Phys. Plasmas*, vol. 17, no. 12, p. 123508, 2010.
- [3] F. Poehlmann-Martins, "Investigation of a plasma deflagration gun and magnetohydrodynamic rankine-hugoniot model to support a unifying theory for electromagnetic plasma guns," Ph.D. dissertation, Dept. Mech. Eng., Stanford Univ., Stanford, CA, USA, 2010.
- [4] C. Lin, H. An, J. Wei, X. Min, W. Shoudong, and L. Ye, "Plasma density measurements in cable gun experiments with a sensitive He-Ne interferometer," *Plasma Sci. Technol.*, vol. 9, no. 3, p. 292, 2007.